

UDC 622.276.53

DOI 10. 56525/KAWV2683

MODEL PREDICTIVE CONTROL FOR ROD PUMP SYSTEMS

Chazhabayeva M.

Yessenov University, Aktau, Kazakhstan

e-mail: marzhan.chazhabayeva@yu.edu.kz

Abstract. This paper enables to accelerate fluid recovery from oil and gas reservoirs by automatically controlling fluid height and bottomhole pressure in wells. Several studies in the literature show a significant increase in recoverable oil by determining a target bottomhole pressure, but rarely consider how to control this value. This work provides these advantages by maintaining bottomhole pressure or fluid elevation. Moving horizon estimation (MHE) determines uncertain well parameters using only conventional surface measurements. A model predictive controller (MPC) adjusts the stroke rate of the rod pump to maintain fluid height. Pump boundary conditions are modeled using mathematical programs with complementarity constraints (MPCC), and a nonlinear programming solver finds a solution in near real time. A combined rod string, well and reservoir model simulates dynamic conditions in the well and is formulated for simultaneous optimization by large-scale solvers. MPC increases cumulative oil production over conventional pump shut-in control by maintaining optimal fluid elevation.

Keywords. Control with model prediction, modeling, rod pumps, gas and oil, MPC, MHE.

Introduction

In the production oil and gas industry, the application of new intelligent automation technologies can increase reservoir recovery and reduce operating costs. Intelligent technologies increase data acquisition, provide real-time data analysis, and improve equipment controllability.

The implementation of maximum benefit from these devices requires the development of system models, automated controllers and automated optimization procedures.

Automation is the foundation of innovation. Automation at a basic level requires three components: 1) a sensor; 2) a controller; and 3) an operator.

In automatic control, first the sensor measures the process variable. Second, based on the measurement and controller configuration, the controller sends output data to the actuator. Finally, the actuator affects the process, resulting in closed-loop automation. As global Internet connectivity expands, the ability to collect measurements from sensors and send control signals to actuators increases. At the same time, the cost of computing devices is decreasing and computational performance is increasing. These factors are driving an automatic revolution in many industries. To maintain competitiveness, oil and gas companies are beginning to adopt automation technologies. An important area of smart technology development is artificial lift systems on suction cups.

Rod pumping is a widely used artificial lift method for the extraction of oil and gas resources. Modern rod pumping technology was developed in 1926 and has remained virtually unchanged since then. In rod pumping, a pump at the bottom of the well is driven by the linear motion of a surface unit up and down a string of rods. As fluids are produced from the formation, the bottomhole pressure (BHP) of the well decreases and the pressure drop between the formation and the well results in the flow of formation fluids into the wellbore. Several literature studies have shown how the ultimate recovery and projected net present value (NPV) increase significantly as a result of optimal fuel management in storage systems [1,2,3].

Well control technologies are currently generating significant interest in the oil and gas industry, primarily because producers can increase estimated ultimate production by 10-15% [4].

As the speed of computers and data gathering systems continues to improve, the industry expects control technologies to become a more integral part of the well life cycle optimization process.

The development of intelligent rod pumping equipment allows well control optimization to be applied in practice in two ways. First, it makes it easy to make optimal adjustments using automatic control. Second, it allows system identification to characterize the correlation between controlled variables (e.g., hp production rate) and system behavior (e.g., fluid production rate) [5].

Research Methods. This article describes the rod pump, well, and reservoir models. It also describes environmental considerations and provides general formulations of the MHE and MPC problems.

Rod pumping is a widely used artificial lift method for producing oil and gas from repeated sources. In rod pumping, a positive displacement pump at the bottom of the well is driven by linear movement up and down the surface unit using a string of rods. One of the problems often encountered with rod pumping occurs when the pump travel speed exceeds the rate at which the flow of fluid from the formation can fill the pump. This results in a mechanical stress known as fluid shock. In this case, the pump barrel partially fills with fluid during the upstroke and then the pump plunger abruptly contacts the fluid in the pump barrel during the down stroke.

Diagnosing pumping conditions such as fluid poundage is challenging because measurements are rarely taken at the pump due to harsh conditions and the inconvenience/cost of installing and maintaining downhole sensors.

To prevent inefficient fluid production and equipment damage, many methods have been developed to detect pump shutdown and control surface installation. With few exceptions, these methods utilize reactive controllers that either adjust the motor speed or simply shut down the rig for some predetermined period of time. One common method of diagnosing pumping conditions is to measure the lift force and position of the surface unit during reciprocating motion of the rod string, and then calculate the corresponding pump force and position based on a model of the rod string system.

The surface measurements are often referred to as polished rod load and polished rod position.

When the load of a polished rod or pump is plotted as a function of position during cycling, it is called a dynamometer chart. The form of the pump dynamometer chart allows the pumping conditions to be diagnosed. Figure 1 shows a typical measured surface map and its corresponding pump design map, where the rectangular shape of the well (pump) map indicates that the pump is filled with fluid. Methods that can automatically diagnose pumping conditions from the shape of the pump dynamometer map require training using datasets and are only suitable for feedback control. To improve the ability to determine BHP and control rod pump systems, this paper proposes an improved control system using a novel combination of rod pump, well and reservoir models. The pump boundary conditions are formulated as mathematical programs with additionality constraints (MPCC), which allows simulation and optimization using simultaneous methods with large-scale solvers. MHE estimates uncertain parameters for control. Advanced controller reduces equipment damage and maximizes fluid production.

Hardware interface for advanced control. One of the smart oilfield devices is the hydraulically driven rod pumping system. The demonstration-sized modular hydraulic rod pumping system shown in Figure 2 includes dynamic measurement of polished rod position and force, motor power consumption or power generation [6]. The main advantage of the hydraulic lifting mechanism is that the stroke of the rod can be adjusted automatically to improve energy efficiency and extend the life of the equipment. Opto22, an industrial control hardware, interfaces with the demonstration unit to transmit measured data to and control signals from the advanced controller. The hardware interfacing with the demonstration unit shows that the advanced control systems shown in this paper can be applied to existing oilfield equipment.

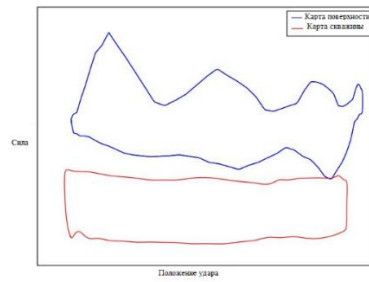


Figure 1 - Illustration of the measured surface dynamogram and the corresponding calculated downhole dynamogram



Figure 2 - Hydraulically driven demonstration rod pump

Wellbore and rod string system. Figure 3a shows a schematic of the wellbore layout. Formation fluid enters the wellbore through a perforation in the casing. Fluid accumulates in the annular space between the casing and production tubing. Figure 3b shows the surface installation of a rod pump adapted from Gibbs [7]. A traction motor drives the rod string in reciprocating motion through a four-rod mechanism. The rod string is connected to a positive displacement pump at the bottom of the well. The pump lifts formation fluid to the surface of the well. When the surface unit raises the pump, the reduced pressure forces fluid into the bottom of the pump unit through a stationary one-way valve (standing valve), filling the pump barrel. When the surface unit lowers the pump, the liquid in the pump barrel flows into the service pipes through another one-way valve (traveling valve). The surface unit makes reciprocating motions of the rod column, and the pump produces fluid with each lift.

Surface unit equations of motion. Equations 1 and 2 describe the vertical position of a conventional four-boom rod pump as a function of the angle of rotation of the driving force, θ . L_1 - L_5 are the unit dimensions shown in Figure 3b from Gibbs [7]. In the same study, the motion of a polished rod under the condition of constant stroke speed (SPM) is modeled.

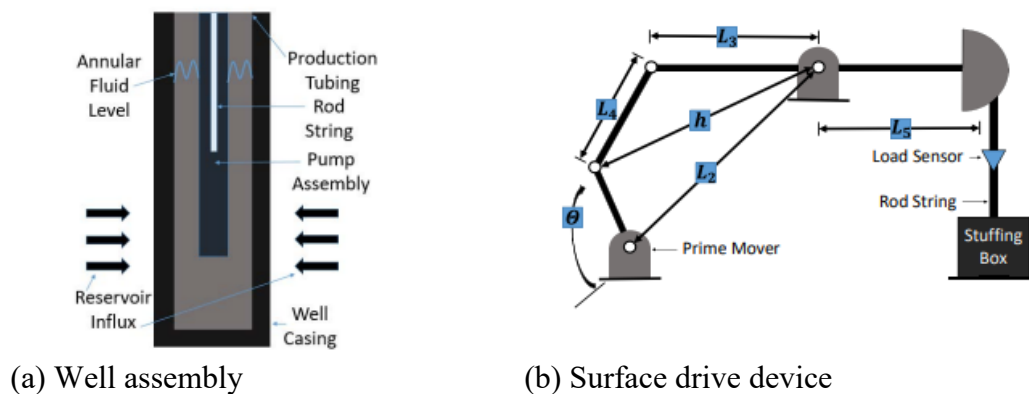


Figure 3 - Pump and well diagrams

To enhance the Gibbs results [7], kinematic equations have been developed for the connecting rod to account for the non-constant EOS. A simplified free body model of a crank arm with non-constant angular velocity is shown in Figure 4. Figure 4 shows three torques acting on the crank arm. These are motor generated torque (T_M), load torque (T_L) and friction torque (T_f). The velocity characteristics of the crank arm with constant angular acceleration can be described by the kinematic equations of rotational motion, Equations 3 and 4. Using Figure 5 and assuming that the hour hand is positive, the torque balance on the center shaft of the crank (point c) is reduced to Equation 5.

$$u(0, \theta(t)) = L_3 \left[\arcsin \left(\frac{L_1 \sin \theta(t)}{h} \right) + \arccos \left(\frac{h^2 + L_3^2 - L_4^2}{2L_3 h} \right) \right] \tag{1}$$

$$h = \sqrt{L_1^2 + L_2^2 + 2L_1 L_2 \cos(\theta(t))} \tag{2}$$

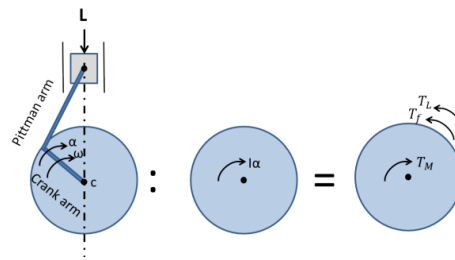


Figure 5 - A free-body diagram of the crank is shown, including a diagram of the acting forces and a diagram of the applied torque

$$\frac{d\theta}{dt} = \omega \tag{3}$$

$$\frac{d\omega}{dt} = \alpha \tag{4}$$

$$\sum M_c = J_0 \alpha = -T_f - T_L + T_M \tag{5}$$

The friction torque in a motor system can be modeled using Equation 6 given in Virgal and Kelemen's paper [8]:

$$T_f = B\omega \tag{6}$$

Equation 6 is a model of the viscous friction torque, which is commonly used as a damping term in electric motor modeling [9]. To simplify the analysis, the load torque and motor torque in Equation 5 are combined into a parameter that we will define as net torque (T_{net}), where $T_{net} = T_M - T_L$. Further, the rotational inertia is assumed to be the total inertia of the motor, the load and gear of the connecting rod, and the load and gear of the rod pump system. Combining equations 3, 5, and 6, the torque balance equation is reduced to equation 7:

$$J_0 = \frac{d\omega}{dt} = -B\omega + T_{net} \tag{7}$$

Rearranging the equation into the standard form, we obtain the equation:

$$\frac{J_0}{B} \frac{d\omega}{dt} = -\omega + \frac{1}{B} T_{net} \tag{8}$$

which reduces to the standard form for a first-order system often found in process control, as shown in the equation 9:

$$\tau \frac{d\omega}{dt} = -\omega + kT_{net} \quad (9)$$

where $\tau = \frac{J_0}{B}$ - is the time constant, $\tau = \frac{J_0}{B}$ - is the system gain. For our analysis, it is convenient to express the dynamic equations in terms of SPM. The angular velocity is related to the SPM by the simple relationship given in Equation 10:

$$\omega = \frac{2\pi}{60} SPM \quad (10)$$

The integration of equations 9 and 10 and solving explicitly for the time derivative leads to the following formula:

$$\frac{dSPM}{dt} = -\frac{1}{\tau} SPM + \frac{60 k}{2\pi \tau} T_{net} \quad (11)$$

Equation 11 is extended to a second-order system by adding an additional equation that relates the SPM to $\frac{d\theta}{dt}$. This can be achieved by combining equations 3 and 10. The result is equation 12:

$$\frac{d\theta}{dt} = \frac{2\pi}{60} SPM \quad (12)$$

Equations 11 and 12 describe the equations of motion of the connecting rod in terms of SPM. They can be synchronized with Equations 1 and 2 to model the surface position of the connecting rod string at non-constant SPM values. The surface position is then translated into the dynamics of the lower rod string segments using the wave equation given in Equation 13.

Rod string and wellbore modeling. The one-dimensional wave equation with viscous damping models the rod string dynamics presented in Equation 13 [7, 10, 11], considering floating gravity effects, and describes the force propagation and motion in the rod string.

$$\frac{\partial^2 u(x,t)}{\partial t^2} = a^2 \frac{\partial^2 u(x,t)}{\partial x^2} - \frac{\pi a V}{2L} \frac{\partial u(x,t)}{\partial t} - \left(1 - \frac{\rho_w \gamma}{\rho_r}\right) g \quad (13)$$

The modeling of the rod column requires two boundary conditions.

First, the position of the polished rod load is specified, as shown in the general case in Equation 14, where $F(t)$ represents an arbitrary motion profile defined by the surface block. In this paper, the kinematic equations for a conventional rod pump are used.

Second, the well pump behavior is modeled by Equation 15, where α , β и $P_{bd}(t)$ depend on the pumping conditions [7]. In this study, it is assumed that the produced fluid is liquid and incompressible. In this case α is 0, β is 1, and $P_{bd}(t)$ is defined by Equation 16. Equation 16 shows that the load on the pump is zero when the pump is down (the liquid column is held by the service pipes) and equal to the buoyant weight of the liquid in the service pipes when the pump is lifted.

$$u(0, t) = F(t) \quad (14)$$

$$P_{bd}(t) = \alpha_p + \beta \frac{\partial u(x_f, t)}{\partial x} \quad (15)$$

$$P_{bd}(t) = \begin{cases} \frac{W_f - (A_t - A_c) P_{wf}}{EA_c} & \text{if: } \frac{\partial u(x_f, t)}{\partial t} > 0.0 \\ 0.0 & \text{if: } \frac{\partial u(x_f, t)}{\partial t} \leq 0.0 \end{cases} \quad (16)$$

The differential form of Hooke's law defines the load on each segment of the rod as shown in Equation 17.

$$f(x, t) = EA_c \frac{\partial u(x, t)}{\partial x} \quad (17)$$

This paper further considers the dynamic effects of the fluid level in the annulus and the inflow of formation fluid. The material mass balance at the well shown in Figure 3a gives Equation 18.

$$\frac{dm}{dt} = \rho_w \gamma (q_{in} - q_{prod}) \quad (18)$$

Where $\frac{dm}{dt}$ is mass change in the borehole ring space, and q_{in} and q_{prod} - inflow of fluid from the reservoir and fluid produced by the pump. q_{in} and q_{prod} are shown in Equations 19 and 23 for incompressible fluids. Equation 19 is piecewise constant since liquid is only removed from the control volume during the pump lift time.

$$q_{prod} = \begin{cases} A_{c_{pump}} \frac{\partial u(x_f, t)}{\partial t} & \text{if: } \frac{\partial u(x_f, t)}{\partial t} > 0.0 \\ 0.0 & \text{if: } \frac{\partial u(x_f, t)}{\partial t} \leq 0.0 \end{cases} \quad (19)$$

Assuming the fluid is incompressible, Equation 18 expands to Equation 20. Simplification leads to the final equation describing the change in fluid height in the borehole ring space, Equation 21. Reformulating Equation 21 into oilfield units yields Equation 22. During the modeling process, equations 13, 14, 19, 21 and 23 are solved simultaneously, which allows dynamic modeling of the well.

$$\rho_f \gamma (A_{c_{casing}} - A_{c_{tubing}}) \frac{dh}{dt} = \rho_w \gamma (q_{in} - q_{prod}) \quad (20)$$

$$\frac{dh}{dt} = \frac{(q_{in} - q_{prod})}{(A_{c_{casing}} - A_{c_{tubing}})} \quad (21)$$

$$\frac{dh}{dt} = \frac{1617}{2} \frac{(q_{in} - q_{prod})}{(A_{c_{casing}} - A_{c_{tubing}})} \quad (22)$$

Reservoir modeling. The simplified well model considers a dissolved gas reservoir in a pseudo-steady-state regime. To further simplify the analysis, we assume that the gas is held in solution throughout the life of the well, i.e., the oil pressure never drops below the bubble point pressure.

Thus, we do not need to consider more complex dynamics such as two-phase flow and relative permeability in the reservoir. Using the above assumptions, the flow performance relationship for a reservoir is defined by Equation 23 [12].

$$q_{in} = \frac{kh(P - P_{wf})}{141.2 B_0 \mu \left(\frac{1}{2} \ln \frac{4A}{\gamma C_A r_w^2} + S \right)} \quad (23)$$

At pressures above the bubble point, fluid recovery from an oil reservoir depends entirely on the expansion of the fluid as the reservoir pressure decreases. This behavior can be described by the isothermal compressibility defined by equation 24 [13].

$$c = -\frac{1}{V} \frac{\partial V}{\partial P} \quad (24)$$

Integrating Equation 24 by the method of separation of variables from the initial formation pressure to the current average formation pressure, the solution of the equation in partial differentials takes the following form:

It should be noted that c is assumed to be constant throughout the life of the well. The volume at lower mean reservoir pressure \bar{P} includes the volume remaining in the reservoir, V_i , and the volume of produced fluid, V_p , i.e., V_p .

$$\frac{V}{V_i} = e^{c(P_i - \bar{P})} e^{c(P_i - \bar{P})} \quad (25)$$

It is worth mentioning that c is assumed to be constant throughout the life of the well. The lower mean reservoir pressure \bar{P} includes the volume remaining in the reservoir, V_i , and the volume of fluid produced, V_p , i.e., V_p .

$$V = V_i + V_p \quad (26)$$

By combining equations 25 and 26, an explicit solution can be obtained for the average reservoir pressure as a function of the total volume extracted from the reservoir, as shown in the equation 27:

$$\bar{P} = P_i - \frac{1}{c} \ln \left(\frac{V_p}{V_i} + 1 \right) \quad (27)$$

The total volume produced is determined by the equation 28:

$$V_p = \int q_{out} dt \quad (28)$$

Using equations 23, 27, and 28, it is possible to develop a model for the dependence of reservoir inflow capacity (IPR). The values of the constants given in the equations are given in the nomenclature section.

Conclusion. The groundbreaking contribution of this work is as follows:

1. The Moving Horizon Estimation (MHE) application evaluates uncertain well and reservoir parameters or variable states using only commonly measured data from pumping rod systems. These estimates are made almost in real time, which allows you to automatically control the height of the annular space of the well. This development also reduces the need to stop production to perform pressure boosting tests or determine well parameters. These tests are time-consuming and costly.

2. A combined model of a rod pump, well and reservoir. Model Predictive Control (MPC) uses a combined model to optimally determine well parameters and directly account for the physical limitations of the system.

REFERENCES

1. M. Cardoso and L. Durlofsky. Use of Reduced-Order Modeling Procedures for Production Optimization. SPE Journal, 15(2):1–10, 2010.
2. Z. M. Alghareeb. Optimal Decision Making in Reservoir Management Using Reduced Order Models. In SPE Annual Technical Conference and Exhibition held in New Orleans, Louisiana, 2013
3. J. He, P. Sarma, and L. J. Durlofsky. 1. Use of reduced-order models for improved data assimilation within an EnKF context. In SPE Reservoir Simulation Symposium, page 2014, 2014.
4. M. Islam, S. Moussavizadegan, S. Mustafiz, and J. H. Abou-Kassem. Advanced Petroleum Reservoir Simulation. Scriener Publishing LLC, Hoboken, 2010.
5. J. Udy, B. Hansen, S. Maddux, D. Petersen, S. Heilner, K. Stevens, D. Lignell, and J. D. Hedengren. Review of Field Development Optimization of Waterflooding, EOR, and Well Placement Focusing on History Matching and Optimization Algorithms. Processes, 5(3):34, jun 2017.

6. D. A. Krug, S. D. Nelsen, and J. D. Allison. Regenerative hydraulic lift system, oct 2013.
7. S. G. Gibbs. Predicting the Behavior of Sucker-Rod Pumping Systems. Journal of Petroleum Technology, 1963.
8. I. Virgal and M. Kelemen. Experimental Friction Identification of DC Motor. International Journal of Mechanics and Applications, 3:26–30, 2013.
9. P. Wolm, X. Chen, J. Chase, W. Pettigrew, and C. Hann. Analysis of a PM DC Motor Model for Application in Feedback Design for Electric Powered Mobility. Mechatronics and Machine Vision in Practice, 2008.
10. R. M. Knapp. A Dynamic Investigation of Sucker-Rod Pumping. MS thesis, University of Kansas, Topeka, page 46, 1963.
11. T. A. Everitt and J. W. Jennings. An improved finite-difference calculation of downhole dynamometer cards for sucker-rod pumps. SPE Production Engineering, 7(01):121–127, 1992.
12. M. J. Economides, A. D. Hill, C. Ehlig-Conomides, and D. Zhu. Petroleum Production Systems. Prentice Hall, Upper Saddle River, NJ, 2013.
13. W. McCain. The Properties of Petroleum Fluids. PennWell Books, Tulsa, Okla, 1990.

ШТАНГАЛЫҚ СОРҒЫ ЖҮЙЕЛЕРІНЕ АРНАЛҒАН МОДЕЛЬ БОЙЫНША БОЛЖАМДЫ БАСҚАРУ

М.М. Чажабаева

Есенов университеті, Ақтау қ. Қазақстан
e-mail: marzhan.chazhabayeva@yu.edu.kz

Аңдатпа: Бұл жұмыс сұйықтықтың биіктігін және ұңғымалардағы кенжар қысымын автоматты басқару арқылы мұнай және газ қабаттарынан сұйықтықты алуды жеделдетуге мүмкіндік береді. Бірқатар әдеби зерттеулер мақсатты кенжар қысымын анықтау арқылы алынатын мұнай көлемінің айтарлықтай өсуін көрсетеді, бірақ бұл мәнді қалай басқару керектігі сирек қарастырылады. Бұл жұмыс сұйықтықтың қысымын немесе биіктігін ұстап тұру арқылы осы артықшылықтарды алуға мүмкіндік береді. Қозғалмалы горизонтты бағалау (МНЕ) ұңғыманың анықталмаған параметрлерін тек қарапайым беттік өлшемдерді қолдана отырып анықтайды. Болжалды модель (МРС) контроллері сұйықтықтың биіктігін сақтау үшін штангалық сорғының жылдамдығын реттейді. Сорғының шекаралық шарттары математикалық комплементарлы шектеулер (МРСС) бағдарламалары арқылы модельденеді, ал сызықтық емес бағдарламалау шешушісі нақты уақыт режимінде шешім табады. Штангалық бағананың, ұңғыманың және қабаттың аралас моделі ұңғымадағы динамикалық жағдайларды модельдейді және ауқымды шешгіштермен бір уақытта оңтайландыру үшін тұжырымдалады. МРС сұйықтық деңгейінің оңтайлы биіктігін сақтау арқылы сорғыны өшіруді дәстүрлі басқарумен салыстырғанда жинақталған мұнай өндірісін арттырады.

Түйін сөздер: Болжамды модельді басқару, модельдеу, штангалық сорғылар, газ және мұнай, МРС, МНЕ.

МОДЕЛЬ ПРОГНОЗИРУЮЩЕГО УПРАВЛЕНИЯ ДЛЯ ШТАНГОВЫХ НАСОСНЫХ СИСТЕМ

Чажабаева М.М.

Есеновский университет, г. Ақтау Казахстан
e-mail: marzhan.chazhabayeva@yu.edu.kz

Аннотация Данная статья позволяет ускорить извлечение жидкости из нефтяных и газовых коллекторов за счет автоматического регулирования высоты подъема жидкости и забойного давления в скважинах. В нескольких исследованиях, опубликованных в литературе, показано значительное увеличение извлекаемой нефти за счет определения заданного забойного давления, но редко рассматривается вопрос о том, как контролировать это значение. Данная работа обеспечивает эти преимущества за счет поддержания забойного давления или перепада высот жидкости. Оценка подвижного горизонта (МНЕ) определяет неопределенные параметры скважины, используя только обычные поверхностные измерения. Модельный интеллектуальный контроллер (МРС) регулирует частоту хода штангового насоса для поддержания высоты подачи жидкости. Граничные условия насоса моделируются с использованием математических программ с ограничениями взаимодополняемости (МРСС), а программа нелинейного программирования находит решение практически в режиме реального времени. Комбинированная модель колонны штанг, скважины и коллектора имитирует динамические условия в скважине и предназначена для одновременной оптимизации с помощью крупномасштабных решений. МРС увеличивает суммарную добычу нефти по сравнению с обычным управлением при отключении насоса за счет поддержания оптимального уровня жидкости.

Ключевые слова. Управление с помощью модельного прогнозирования, моделирования, штанговых насосы, газ и нефть, МРС, МНЕ.